Complex wave propagation in the Campi Flegrei Caldera, Italy, from source- and receiver-array analysis of sea-shot recordings

V. Nisii and G. Saccorotti

Istituto Nazionale di Geofisica e Vulcanologia - Osservatorio Vesuviano, Napoli, Italy

(Received June 9, 2005; accepted August 9, 2005)

ABSTRACT We investigate wave propagation in the complex shallow crust of Campi Flegrei Volcanic Complex, Italy, using array recordings of air-guns. We apply source- and receiver-array analysis to define the independent variation of horizontal slowness at both the source and receiver regions. This method allows the identification of asymmetric ray-paths associated with near-source and near-observer velocity heterogeneities. P-wave wave-vectors at both the source and receiver arrays depict discrepancies as large as 50° with respect to the values expected for the 3D velocity structure of the Gulf. At the source region, these discrepancies may be associated with either un-modelled complexities in the geometry of the buried caldera rim, or with velocity variations beneath the source-array. At the receiver array, the inferred anomalies may be attributed to velocity variations marking the Solfatara crater rim, or to a near-receiver, low-velocity body whose position would coincide with negative gravimetric anomalies and a low Vp/Vs ratio region inferred by independent geophysical and seismological studies.

1. Introduction

Over the past 20 years, seismic arrays have became increasingly popular for the study of the Earth's structure and earthquake source processes [see Rost and Thomas (2002), for an excellent review of array methods and applications]. The main feature of arrays is the capability of accurately determining the propagation parameters (direction and apparent velocity) of incoming seismic energy. However, azimuth deviations of several degrees from a purely radial direction are typical for most arrays. At a global scale, different studies have reported observations of anomalous effects attributed to lateral heterogeneities in the crust (Lin and Roecker, 1996; Bokelmann, 1995) and in the mantle (Kruger *et al.*, 1996; Scherbaum *et al*., 1997). At a local scale, Kruger and Weber (1992) showed evidence of anomalous ray paths induced by a sedimentary layer beneath the array, and Saccorotti *et al*. (2001) reported significant (up to 180°) ray bending due to marked velocity heterogeneities in the near-receiver field. Following the reciprocity theorem, multichannel methods can be extended to single-station recordings of closely-spaced sources, thus allowing us to reveal the details of wave propagation in the near-source field. For instance, Spudich and Bostwick (1987) used a cluster of closely-spaced earthquakes as a source array to study the multiple scattering phenomena in the aftershocks region of the 1984 Morgan Hill (California) earthquake. Goldstein *et al*. (1992) used a source array of nuclear explosion to model the wave propagation and the structure of the upper mantle beneath central Eurasia. For the special case of a multichannel system recording data from a

cluster of sources, array processing schemes may be applied to the simultaneous determination of the wave vectors at both the source and receiver arrays, and to detect secondary sources located throughout the ray-path. Using a cluster of nuclear explosions in Kazakhstan, recorded at the Yellowknife array in northern Canada, Sherbaum *et al*. (1997) detected scatterers and velocity anomalies ranging from the core-mantle transition zone up to 500 km into the lowermost mantle beneath the Arctic Sea region. A well-located cluster of deep events recorded by a receiver array in Australia was used by Kruger *et al.* (2001) to delineate important constraints about heterogeneities of the deep mantle and the subducted lithosphere below the 660 km discontinuity in the Mariana subduction zone.

For all the cases mentioned above, however, major uncertainties arose from the approximate knowledge of hypocenter coordinates and origin times and, in the case of earthquake sources, different focal mechanisms between events and complex source time functions.

In this paper, we use source- and receiver-array analysis to describe asymmetric ray-paths associated with upper crustal heterogeneities in the Campi Flegrei volcanic complex, Italy. We apply the multiple signal classification (MUSIC) technique to a selected set of air-gun sea-shot recordings acquired by a dense receiver array deployed in the centre of the Campi Flegrei caldera. The recordings of sea-shots are ideal for such analysis because the source parameters are well defined. At both the source and receiver regions, we find P-wave back-azimuth anomalies of up to 50° with respect to the values expected for the 3D velocity model obtained from P-wave travel-times inversion by Zollo *et al*. (2003).

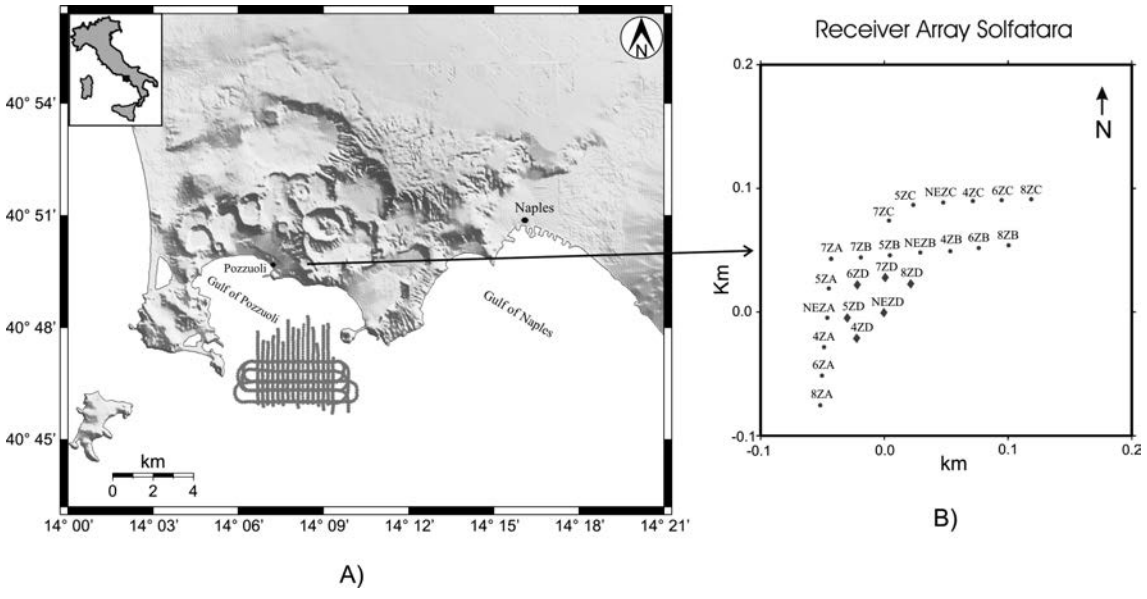

Fig. 1 - (a) Map of the Campi Flegrei showing the experimental layout in the study area. Sea-shots in the Gulf of Pozzuoli are marked by gray circles. (b) Configuration of the array deployed in the Solfatara crater. The gray diamonds indicate the stations selected for receiver array analysis.

1.1. The Campi Flegrei volcanic complex

Located in the Campanian Plain (southern Italy), the Campi Flegrei volcanic complex is a graben-like structure at the eastern margin of the Tyrrhenian Sea, in correspondance to a marked lithospheric thinning, originated during the Pliocene extension phase (Fig. 1a). The recent structure is characterized by many sparse craters and nested calderas associated with different eruptive events, the most important of which produced the Campanian Ignimbrite (about 37-39 ky: Civetta *et al*., 1997) and the Neapolitan Yellow Tuff (about 12 ky: Orsi *et al*., 1996). Resulting from this complex volcanic evolution is a highly heterogeneous crust, as evidenced by the complicated morpho-structural systems, dominated by two concentric segmented caldera rings. Seismological evidence for crustal heterogeneities and laterally-varying P-wave velocity structure were first presented by Finetti and Morelli (1974), from seismic reflection data in the Gulf of Pozzuoli. These authors identified the presence of numerous faults and buried volcanic banks. A recent reprocessing of that data set indicates a strong control of the regional structural discontinuities on the caldera collapse mechanism (Bruno, 2004). An highly-heterogeneous crust results also from the 3D tomographic images of the velocity field (Zollo *et al*., 2003) and distribution of scatterers (Tramelli *et al.*, 2005).

2. Instruments and data

In this study, we use data from a marine-active seismic survey carried out in the Gulf of Pozzuoli during the month of September 2001 (Zollo *et al*., 2003). The sources consisted of shots from synchronized air-guns; the shooting layout was designed to provide a very high data density throughout the gulf, where about 2500 shots were fired along a grid pattern with N-S and E-W lines spanning an exploring surface of about 5 by 5 km. The distance between adjacent shot lines was about 125 and 250 meters along the N-S and E-W directions, respectively (Fig. 1a).

During this survey, the Osservatorio Vesuviano (INGV) and the Instituto Andaluz de Geofisica at the University of Granada (Spain) deployed a dense array of seismometers in the Solfatara crater, about 2 km east of the harbour of Pozzuoli (Fig. 1a). This array consisted of 20 vertical-component and 4 three-component seismometers arranged in a triangular pattern with aperture of about 250 m and average inter-station spacing of about 25 m (Fig. 1b). All seismometers had a natural frequency of 4.5 Hz, electronically extended to 1 Hz. Recording was achieved via PC-based systems with a dynamic range of 16-bit recording data at 200/samples/second/channel. Absolute timing was provided via synchronisation to the GPS time signal. GPS was also used to get the absolute positions of both the sea-shots and receiver-array elements, with an estimated precision of ±10 m and ±10 cm, respectively. Preliminary examination of recordings from the receiver array indicated a dramatic loss of signal coherency for inter-station distances larger than about 100-150 m. Due to this reason, we conducted the analysis at the Solfatara array using only data from the 6-element sub-array D, whose aperture and average receiver spacing were in the order of 60 m and 20 m, respectively. An example of a 3 km distant sea-shot recording is illustrated in Fig. 2.

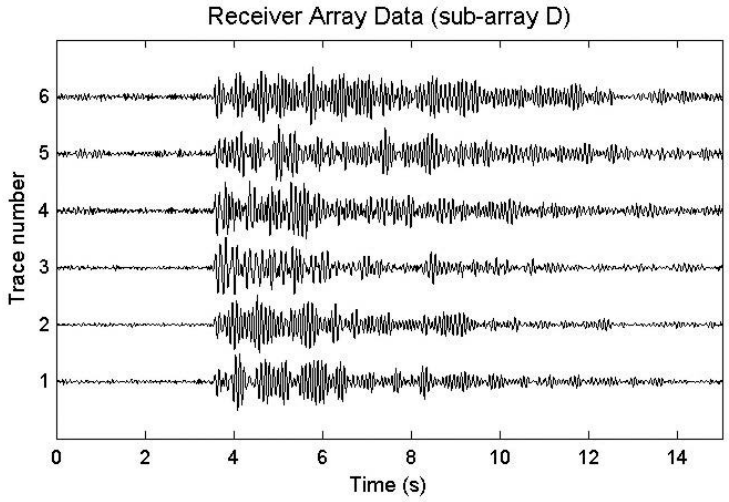

Fig. 2 - Ground velocity recordings of a sea-shot from the vertical sensors of sub-array D (gray diamonds in Fig. 1). Origin time is at zero second in the time scale. The data are unfiltered.

3. Method of analysis

The propagation parameters (slowness vector) at both the source and receiver arrays are estimated using MUSIC, the MUltiple Signal Classification technique (Schmidt, 1986; Goldstein and Archuleta, 1991). Once compared to more classical array-processing methods, MUSIC demonstrates superior detection performances under poor SNR conditions, and exceptional resolving capabilities toward multiple signals simultaneously impinging at the array.

For a given data window recorded by an *N*-element array, the estimate of the MUSIC slowness spectrum begins with the evaluation of the spatial covariance of the signal, parameterized through the *N* by *N* cross-spectral matrix (CSM). Applying Akaike's information criterium (Wang and Kaveh, 1985) to the sorted eigenvalues of the CSM, we then estimate the rank of the signal subspace, i.e. the number of signals *M* impinging at the array. The slowness spectrum is eventually obtained as :

$$Q(\vec{s}) = \frac{1}{1 - \sum_{i=1}^{M} \left| A(\vec{s}) \cdot V_i^2 \right.} , \qquad (1)$$

where V_i is the *i-th* signal eigenvector of the CSM and $A(\vec{s})^H$ is the Hermitian of an *N* by 1 column vector containing the expected inter-station phase shifts for a monochromatic plane-wave of frequency ω_0 propagating with slowness $\vec{s}$. The elements of vector A($\vec{s}$) are defined as:

$$A(\vec{s}) = \frac{1}{\sqrt{N}} \begin{pmatrix} e^{i\omega_0 \vec{s} \cdot (\vec{x}_i - \vec{x}_0)} \\ \vdots \\ e^{i\omega_0 \vec{s} \cdot (\vec{x}_i - \vec{x}_0)} \end{pmatrix}, \qquad (2)$$

where $\vec{x}_i$ and $\vec{x}_0$ are the position vectors of the *i-th* and reference receivers, respectively.

Maximising the directional function $Q(\vec{s})$ [Eq. (1)] thus means finding those slownesses for which the vector $A(\vec{s})$ has a maximum projection onto the signal subspace spanned by the $i=1, \ldots M$ eigenvectors V_i. Peaks in the slowness spectrum $Q(\vec{s})$ are then associated with the horizontal slownesses of individual plane-wave components impinging the array. The amplitude of these peaks is completely uncorrelated to the actual amplitude of the signal, and only gives a measure of the consistency with which the observed inter-stations phase delays fit the model of a plane-wave propagating at the particular slowness $\vec{s}$.

3.1. Uncertanties estimation

The standard approach for estimating slowness precision is to assume that peaks in the power spectrum have been shifted by some small amount due to the combined effects of noise and systematic timing variations associated with velocity heterogeneities beneath the array. Under this simplifying hypothesis, we evaluate the precision of our slowness estimates using the relationship (Goldstein and Archuleta, 1991):

$$\sigma_{\vec{s}} \approx \sqrt{\left(\frac{\partial t}{\sqrt{N}\Delta x}\right)^2 + \left(\frac{\sqrt{1 + N_s \cdot SNR}}{N_s \cdot SNR \cdot \sqrt{M}\, 2\pi L f}\right)^2}\,, \tag{3}$$

where N_S is the number of array elements, M is the number of samples in the window of analysis, f is the frequency, L is the aperture of the array, Δx is the average sensor spacing and δt is the uncertainty in delay times between array elements. For a given estimate of ray parameter $|\vec{s}|$ and associated uncertainty $\sigma_{\vec{s}}$, the corresponding error in the azimuth estimate σ_ϕ is then given by (Saccorotti *et al*., 1998):

$$\sigma_\phi \approx \tan^{-1}\left(\frac{\sigma_{\vec{s}}}{|\vec{s}|}\right). \tag{4}$$

In the uncertainty analysis we considered reference values of frequency and a ray parameter of 8 Hz and 0.25 km/s, respectively, and SNRs varying between 20 to 50 in order to account for the different quality of the data associated with variable source-to-receiver distances. For the source-array case, we assume δt = 0.05 s, Δx = 100 m, L = 750 m and N_S = 6 or 9, yielding ray parameter and azimuth uncertainties of about 0.2 km/s and 30°, respectively. In the case of the receiver array, the array aperture and average sensor spacing are much lower than the dominant wavelength of the signal: therefore, we set the delay time uncertainty equal to the sampling rate. By further setting Δx = 20 m, L = 60 m and N_S = 6, we finally get ray parameter and azimuth uncertainties of about 0.1 km/s and 20°, respectively.

An example of MUSIC analysis is displayed in Fig. 3, which reports the results of receiver array analysis 1 showed in Fig. 4.

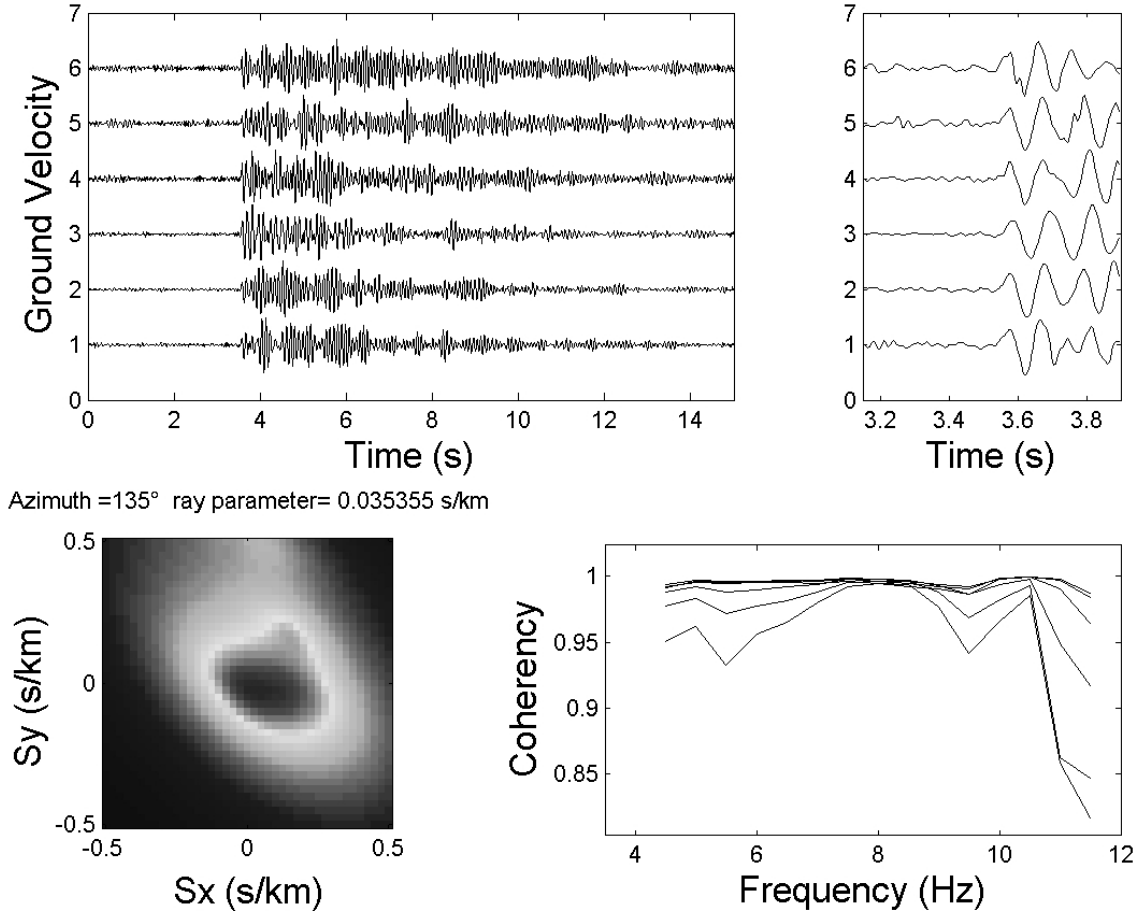

Fig. 3 - (a) vertical-component recordings at the Solfatara receiver array associated with shot 1 (see Fig. 4); (b) time interval used for P-wave slowness analysis; (c) time-frequency stacked slowness spectrum. The title indicates azimuth and ray parameter associated with the main peak; (d) multichannel signal coherency over the frequency band selected for the analysis. Each line refers to the different time windows used for the analysis.

4. Double array analysis

Following Green's function reciprocity theorem, we apply the source-array analysis to a selected data set constituted by 9 clusters of 6-9 sea-shots recorded at the reference receiver NEZD (Fig. 1b). The receiver array analysis is conducted over 9 of these shots, recorded by receiver array D deployed in the Solfatara crater (see Fig. 4).

We first conducted a preliminary analysis of the spectral content of the data in order to finely tune the parameters of the MUSIC technique. The shot recordings depict a narrow spectrum, with most of the energy concentrated within the 6-10 Hz frequency band.

The first step of the analysis then consists in passing the array signals through a bank of narrow (1.5 Hz bandwidth) zero-phase-shift band-pass filters centred respectively on these frequency: 4.75 Hz, 6.25 Hz, 7.75 Hz, 9.25 Hz, 10.75 Hz. From the Hilbert transform of the filtered traces we obtain the analytic signals, which are eventually used to get the complex-valued

estimates of the narrow-band spatial covariance matrix. Using SVD, we derive the eigenvalues and eigenvectors of this matrix, and proceed with the evaluation of the number of signal and the slowness spectrum $Q(\vec{s})$ of Eq. (1) above. The procedure is repeated over six, 1-s-long time windows overlapping by 80% of their length and encompassing the first P-wave arrival. The calculations are then iterated over the different reference frequencies, and a final slowness spectrum is derived from the stack of individual spectral estimates obtained over the different time intervals and frequency bands. Stacking the slowness spectra evaluated at different reference frequencies has the effect of enhancing the contribution of body-waves, in turn attenuating the effects of spatial aliasing and dispersive arrivals both of which depend on frequency (Spudich and Oppenheimer, 1986).

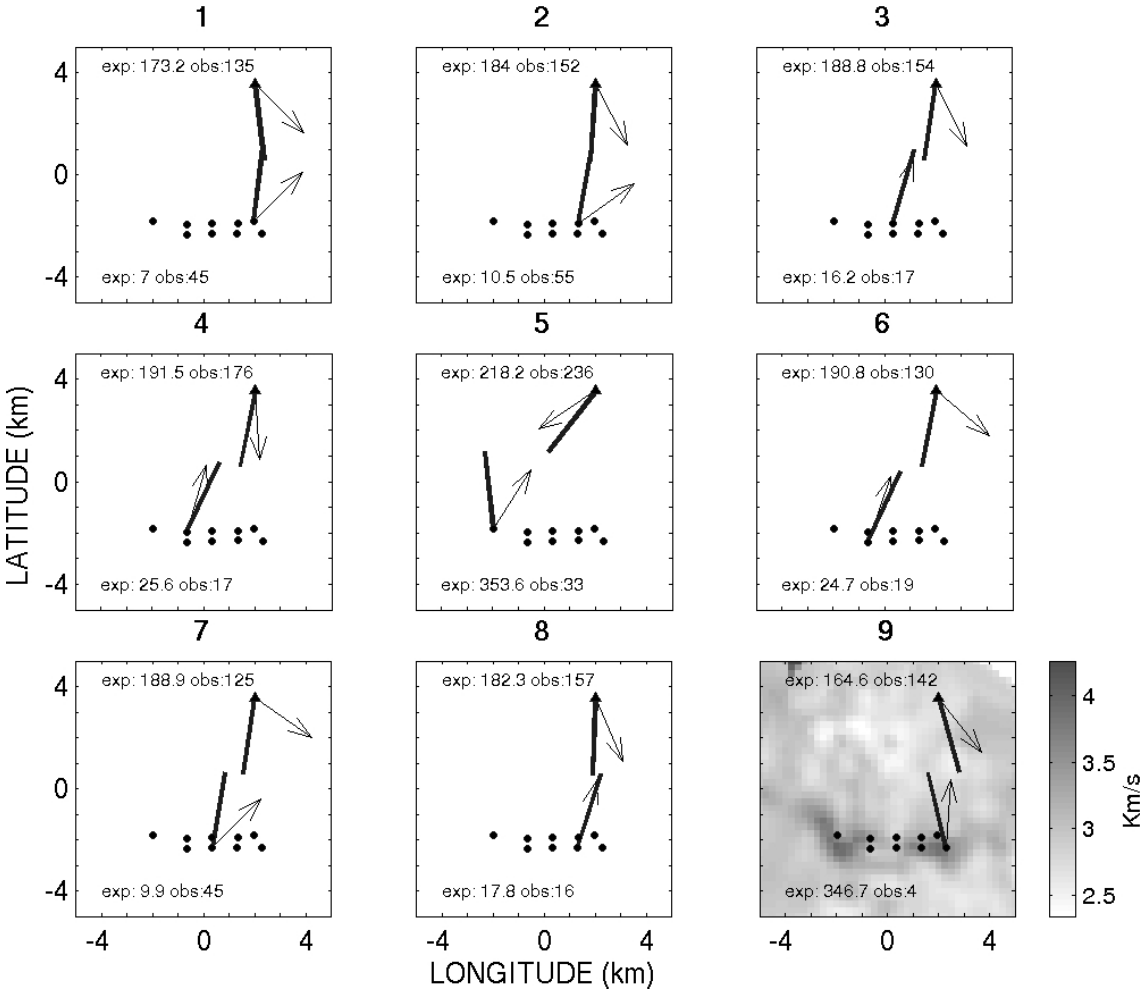

Fig. 4 - Plots illustrating the observed (arrow) and the theoretical backazimuths (bold line) obtained for each source-receiver pair. The triangle indicates the receiver-array position, while the circles depict the reference source-array positions. The image map in the analysis number 9 depicts the velocity model section at 1.25 km depth extrapolated from the 3-D tomographic image by Zollo *et al.* (2003). The gray bar indicates P-wave velocity.

Estimating the slowness vectors at both the source and receiver arrays allows the retrieval of the propagation parameters (propagation azimuth and apparent velocity) associated with the initial and final paths of the seismic rays. For most of the source- and receiver-array pairs, azimuths and ray parameters obtained from our analysis are generally discrepant with those expected for a flat-layered Earth model. These discrepancies are however difficult to assess for what concerns ray parameters, as the typical value we got (ranging between 0.03 and 0.2 s/km) has the same order of magnitude as the associated uncertainties. Azimuthal data instead are more significant, even accounting for measurement errors once. Fig. 4 illustrates the backazimuths obtained from the double array analysis. Using the finite-difference method of Podvin and Lecomte (1991), we then calculated the expected backazimuth angles for the 3D model of Zollo *et al*. (2003). Backazimuths measured at the source array depict a complicated pattern, deviating significantly from the expected values. The most prominent feature is a marked NE deflection associated with sources located in the central sector of the gulf (source arrays 1, 2 and 7), an effect which attenuates as one moves towards the westernmost sources, where quasi-radial wave-vectors are observed instead. As expected, the largest anomalies are associated with the region of greatest velocity gradients, i.e. at the positive anomaly detected by Zollo *et al.* (2003) in the central sector of the gulf. A similar pattern is observed at the receiver array, where back-azimuths associated with shots 02, 03, 06, 07, 08 and 09 depict SE deflections of up to about 60° with respect to the theoretical value.

5. Discussion and conclusions

In this paper we presented an application of multichannel methods to analyse the propagation of seismic waves in the complex structures marking the caldera of the Campi Flegrei volcanic complex, Italy. The double array analysis performed using the MUSIC technique revealed a complex geometry of raypaths: we found azimuthal discrepancies as large as 50° with respect to the values predicted using the 3D model of Zollo *et al*. (2003) at both the near-source and near-receiver regions. These observations thus point to the existence of marked heterogeneities not revealed by the 3D tomographic imaging based on travel time inversion. Our data have dominant wavelengths on the order of 300-500 m. Thus, in principle, the 250-m resolution featured by the 3D tomographic model for the shallowest 2 km of crust (Zollo *et al*., 2003) should provide sufficient approximation for the prediction of ray paths. However, at either the initial or terminal part of ray-paths, velocity variations have a much larger effect on ray geometry than on travel times [see Fig. 1 in Hu *et al*. (1994)].

Therefore, we expect that the aforementioned discrepancies represent the effect of small-scale velocity gradients not resolved by the travel-time tomography. Moreover, for the large velocity gradients pinpointed beneath the source arrays, the fundamental assumption of plane-wave propagation may be violated, as the widely-spaced elements of the source arrays could span regions of not-uniform velocity.

In this framework, the anomalies detected at the source arrays may be interpreted as un-modeled complexities in the geometry of the high-velocity body already interpreted by Zollo *et al*. (2003) as buried remnants of the largest Neapolitan Yellow Tuff caldera rim. The striking discrepancies observed at the receiver array have, instead, a twofold interpretation. They could in

fact be due to a severe ray bending associated with the velocity contrast which is expected at the boundary between the inner and outer parts of the Solfatara Crater. Alternatively, one could invoke the presence of a low-velocity region located S-SW of the Solfatara Crater, the effects of which would be an eastward bending of seismic rays impinging at the array from S-SW. There is correlation between this observation and the position of the high Vp/Vs anomaly revealed by Aster and Meyer (1988) and by Vanorio *et al*. (2005) at about a 1 km depth. In addition, the position of the inferred anomaly would also be associated with the area where the maximum uplift and seismicity rate were observed during the last bradyseismic crisis (1982-1984), in turn coinciding with a strong scattering body imaged through a recent 3-D local-earthquake scattering tomography (Tramelli *et al*., 2005).

With the data presently available, it is impossible to gain further insights about location and size of any such anomalies. Slowness vectors respond to uncertainties in the velocity gradient and are therefore best suited for delineating the edges of velocity anomalies. Future studies will therefore aim at extending the source array analysis using recordings from the stations of the sparse network deployed during the experiment, in order to retrieve a detailed image of the velocity heterogeneities scanning the central part of the gulf from inversion of wavevectors (e.g., Hu *et al*., 1994).

Aknowledgements. Aldo Zollo and coworkers are greatly acknowledged for having provided their 3D velocity structure. The multichannel instrumentation was made available by Jesus Ibanez and Miguel Abril; Javier Almendros and Enrique Carmona provided a constant helping hand during the array deployment and maintenance. Edoardo Del Pezzo is sincerely acknowledged for the many helpful comments and suggestions provided during the preparation of the manuscript. This work is part of the project of the Regional Center of Competence "Analysis and Monitoring of the Environmental Risk" (AMRA) supported by the European Community, and has been partially supported through EU grants *SERAPIS* and *e-Ruption*.

REFERENCES

Aster R. and Meyer R.; 1988: *Three-dimensional velocity structure and hypocenter distribution in the Phlegrean Fields, Italy.* Tectonoph., **149**, 195-218.

Bokelmann G.H.R.; 1995: *Azimuth and slowness deviations from the GERESS regional array*. Bull. Seism. Soc. Am., **85**, 1456-1463.

Bruno P.P.; 2004: *Structure and evolution of the Bay of Pozzuoli (Italy) using marine seismic reflection data: implications for collapse of the Campi Flegrei caldera*. Bull. Volcanol., **66**, 342-355.

Civetta L., Orsi G., Pappalardo L., Fischer R.V., Heiken G. and Ort M.; 1997: *Geochemical zoning, mingling, eruptive dynamics and depositional processes the campanian ignimbrite, Campi Flegrei caldera*. J. Volcanol. Geoth. Res., **75**, 183-219.

Finetti I. and Morelli C.; 1974: *Esplorazione sismica a riflessione dei Golfi di Napoli e Pozzuoli*. Boll. Geof. Teor. Appl.,**16**, 122-175.

Goldstein P. and Archuleta R.J.; 1991: *Deterministic frequency-wavenumber methods and direct measurements of rupture propagation during earthquake using a dense array*. J. Geophys. Res., **96**, 6173-6198.

Goldstein P., Walter W. and Zandt G.; 1992: *Upper mantle structure beneath central Eurasia using a source array of nuclear explosions and waveforms at regional distances*. J. Geophys. Res., **97**, 14097-14113.

Hu G., Menke W. and Powell C.; 1994: *Polarization tomography for Pwave velocity structure in southen California*. J. Geophys. Res., **99**, 15245-15256.

Kruger F. and Weber M.; 1992: *The effect of low velocity sediments on the mislocation vectors of the GRF array.* Geophys. J. Int., **108**, 387-393.

Kruger F., Baumann M., Sherbaum F. and Weber M.; 2001: *Mid mantle scatterers near the Mariana slab detected with a double array method*, Geophys. Res. Lett., **28**, 667660.

Kruger F., Scherbaum F., Weber M. and Schlittenhardt J.; 1996: *Analysis of asymmetric multipathing with a generalization of Double-Beam Method*. Bull. Seism. Soc. Am., **86**, 737-749.

Lin C. and Roecker S.W.; 1996: *P-wave backazimuth anomalies observed by a small-aperture seismic array at Pinyon flat, southern California: implications for structure and source location*. Bull. Seism. Soc. Am., **86**, 470-476.

Orsi G., De Vita S. and Di Vito M.; 1996: *The restless, resurgent Campi Flegrei nested caldera (Italy): constraints on its evolution and configuration*. J. Volcanol. Geoth. Res., **74**, 179-214.

Podvin P. and Lecomte I.; 1991: *Finite difference computation of traveltimes in very contrasted velocity models: a massively parallel approach and its associated tools.* Geophys. J. Int., **105**, 271-284.

Rost S. and Thomas Ch.; 2002: *Array Seismology: Methods and Applications.* Rev. of Geophys., 10.1029/2000RG000100, 2002.

Saccorotti G., Chouet B., Martini M. and Scarpa R.; 1998: *Bayesian Statistics applied to the location of the source of explosions at Stromboli Volcano, Italy*. Bull. Seism. Soc. Am., **88**, 1099-1111.

Saccorotti G., Almendros J., Carmona E., Ibanez J. and Del Pezzo E.; 2001: *Slowness anomalies from two dense seismic arrays at Deception Island Volcano, Antarctica*. Bull. Seism. Soc. Amer., **91**, 561-571.

Schmidt R.O.; 1986: *Multiple emitter location and signal parameter estimation*. IEEE Trans. Ant. Prop., **34**, 276-280.

Sherbaum F., Kruger F. and Weber M.; 1997: *Double beam imaging : Mapping lower mantle heterogeneities using combinations of source and receiver arrays*. J. Geophys. Res., **102**, 507-522.

Spudich P. and Botswick T.; 1987: *Studies of the seismic coda using an earthquake cluster as a deeply buried seismograph array*. J. Geophys. Res., **92**, 10526-10546.

Spudich P. and Oppenheimer D.; 1986: *Dense seismograph array observations of earthquake rupture dynamics.* In: Das S., Boatwright J. and Scholz C. (eds), Geophysical Monograph 37, American Geophysical Union, pp. 285-296.

Tramelli A., Del Pezzo E., Bianco F. and Boschi E.; 2005: *3-D scattering image of the Campi Flegrei caldera (Southern Italy). New hints on the position of the old caldera*rim. Physics of the Earth and Planetary Interiors, submitted.

Vanorio T., Virieux J., Capuano P. and Russo G.; 2005: *Three-dimensional seismic tomography from P wave and S wave microearthquake travel times and rock physics characterization of the Campi Flegrei Caldera.* J. Geophys. Res., **110**, B03201, doi:10.1029/2004JB003102.

Wang H. and Kaveh M.; 1985: *Coherent signal-subspace processing for the detection and estimation of angles of arrival of multiple wide-band sources*. I.E.E.E. Trans. ASSP, **33**, 823-831.

Zollo A., Judenherc S., Auger E., D'Auria L., Virieux J., Capuano P., Chiarabba C., de Franco R., Makris J., Michelini A. and Musacchio G.; 2003: *Evidence for the buried rim of Campi Flegrei caldera from 3-d active seismic imaging*. Geophys. Res. Lett., **30**, doi:10.1029/2003GL018173.

Corresponding author: Vincenzo Nisii
Istituto Nazionale di Geofisica e Vulcanologia - Osservatorio Vesuviano
Via Diocleziano, 328 - 80124 Napoli
phone +39 081 6108327; fax: +39 081 6108351; e-mail: nisii@ov.ingv.it